Pergamon

Int. J. Heat Mass Transfer. Vol. 41, No. 10, pp. 1189–1197, 1998

Printed in Great Britain
0017–9310/98 $19.00+0.00

PII: S0017-9310(97)00218-4

Heat transfer to bubbles under a horizontal tube

KEITH CORNWELL† and I. A. GRANT

Department of Mechanical and Chemical Engineering, Heriot–Watt University, Edinburgh, U.K.

(*Received* 20 *September* 1996 *and in final form* 18 *July* 1997)

Abstract—The mechanisms of boiling heat transfer on the outside of a horizontal tube are multifarious and include contributions from site nucleation, micro-layer evaporation and liquid disturbance. Previous work has shown the strong influence of sliding bubbles which disturb the liquid and can leave a thin evaporating layer under the bubble. Results of experiments designed to determine the local temperature profiles around individual bubbles in water as they slide around the periphery of a thin downward-facing curved surface are presented. High-speed video recording of thermochromic paint on the surface followed by hue analysis and processing allowed detailed examination of a small section of the curved surface. The strong influence of liquid disturbance around the bubble on the local heat transfer is demonstrated. Under the low heat flux conditions of the experiments, the liquid layer under the bubble was found to dry out yielding a high-temperature spot which was quenched by the surrounding liquid when the bubble moved away. © 1998 Elsevier Science Ltd.

1. INTRODUCTION AND AIM

Much of the heat transfer which occurs when boiling on the outside of tube bundles under the low heat flux conditions used industrially is due to bubbles which slide around the tubes rather than those that nucleate on the surface. In previous experimental work at Heriot–Watt University (Cornwell [1] and Cornwell *et al.* [2]), the contribution of sliding bubbles to the heat transfer under boiling and condensing conditions was determined. Based on this work, it was postulated that heat transfer was largely due to the presence of a thin layer of liquid left under the bubble as it translated along the surface.

However more recent work [3] including heat flow to air bubbles under similar conditions has shown that the disturbance effects alone due to the bubbles movement yielded about a third of the heat transfer. This bubble-sweeping effect is the basis of analytical models reported by Nashikawa *et al.* [4] and Tong *et al.* [5]. The work of Kenning and Yan [6] at Oxford University using thermochromic paint and hue analysis of boiling under an inclined plate also indicates sizeable contributions due to turbulence around and behind the sliding bubble. In an attempt to unravel the mechanisms of heat transfer under a tube, the thermographic methods developed at Oxford are adapted here for use under a curved surface. This allows detailed examination of individual bubbles as they flow around the periphery of the tube rather than reliance on mean values over the whole task.

The aim of this work is to determine whether or not a thin layer exists under the bubble and to examine the influence of mechanisms due to liquid disturbance and evaporation on the local heat transfer. This is achieved by studying two sequences of video recording in some detail using visual examination together with hue analysis of a thermochromic coating to determine the surface isotherms.

2. EXPERIMENTAL RIG AND PROGRAMME

In order to examine the local heat transfer coefficients rather than the mean values, it was necessary to adapt the thermochromic technique and hue analysis developed at Oxford to sliding bubbles on a downward facing curved surface. In our case, this involved simulating the horizontal tube by a thin curved-metal shim and arranging for high-speed video recording of both the bubbles outside the shim and their thermal imprint on the inside.

Initially an attempt was made to adapt one of the tubes of a horizontal tube bank used in the work described earlier [1], but this proved difficult owing to the confined space available and a simple rig with a larger and more accessible tube surface was constructed. This rig, shown in Fig. 1, consists of a horizontal half-cylinder of 50 mm diameter and 25 mm length formed from a stainless-steel shim of 0.0254 mm thickness. This half-cylinder is situated at the upper surface of a Perpex-sided cell which contains the working fluid and is arranged so that the shim can be electrically heated from a low-voltage d.c. source. A mirror is situated outside the cell so that high-speed video camera (HSVC) recording of both the inner and outer sides of the curved shim is possible. For tests using Flutec PP1, a small reflux condenser was fitted to the cell. Vapour bubbles were produced by a small heater under the shim or by nucleation on the surface. When mean heat transfer (rather than local) values

† Author to whom correspondence should be addressed.

NOMENCLATURE

A	area [m^2]	r	radius [m]
k	thermal conductivity [kW mK^{-1}]	T	temperature [K].
q	heat flux [kW m^{-2}]	Subscripts	
q_g	heat generated per unit volume [kW m^{-3}]	c	contact
		sat	saturation.

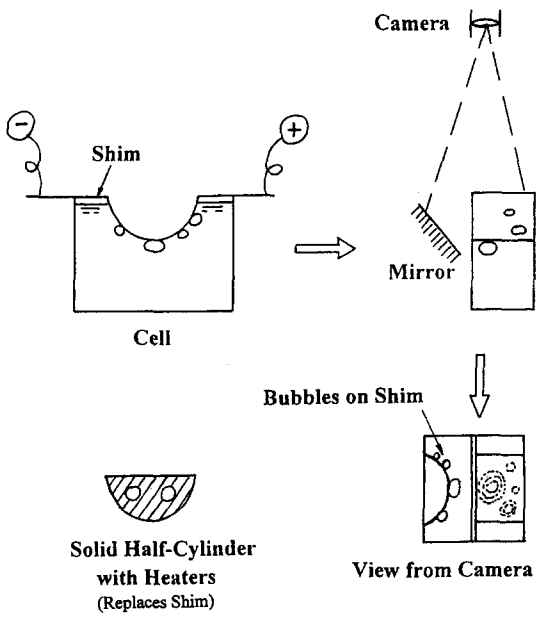

Fig. 1. Arrangement of Perspex cell containing the downward facing cylindrical shim.

were required, the shim was replaced by a solid half-cylinder containing electrical cartridge heaters and thermocouple inserts. Air for the bubbling air tests was produced at a small tube under the half-cylinder.

The inner surface of the shim was coated with a commercial (Radio Spares, UK) thermochromic paint suitable for the temperature range of the heating surface. Paints were available for the required range for boiling water and Flutec PP1 (b.p. 57°C) but not R113, which had been used in our previous work and is now considered environmentally unacceptable. The coating of the paint in a smooth layer on the curved surface proved highly problematic and the best solution was found to be application by brush once the operator had developed the necessary skills. Owing to the camera viewing angle, only a small sector of about 25° each side of centre was able to be examined with reasonable accuracy. The video tape includes a simultaneous record of the physical bubbles and also the colours of the surface on the inside of the shim. The colours were analysed at Oxford University using the same methods as those described in ref. [6], but with an adaption to compensate for the slight curvature involved. Thus, the video signal was transformed into a RGB (red, green, blue) signal and then into a HSI (hue saturation intensity) digitized image which was compared to the hue of the calibrated test sample and recorded as a surface temperature. The resolution was insufficient to allow determination of the local heat flux values as proved possible with the flat surface.

With the possibility of fast-moving bubbles under the curved surface, it was decided to ascertain the influence of the thermal inertia of the shim on the thermal imprint of the bubble. A forward-stepping finite-difference solution to the transient problem was devised and applied to the surface under typical boiling conditions in water. Figure 2 is a typical plot from this analysis and shows the metal shim temperature profiles on one side of a bubble of 5 mm diameter moving steadily along the surface (with centre line at 2.0 mm) at a steady velocity of 20 mm s^{-1}. The heat transfer coefficient under the bubble is taken as (the experimentally reasonable) value of 55 kW m^{-2} K, while elsewhere the value is 0.45 Kw m^{-2} K. The generated heat flux in the metal is 200×10^3 kW m^{-3} (25 A through the shim) and ΔT is 11.3°C. Figure 3 shows the approximate temperature profile along the centre line of the bubble at different bubble velocities. At the velocities encountered in our experiments of up to 20 mm s^{-1}, the influence of the shim extends to about 5 mm behind the bubble and this needs to be borne in mind when examining the images.

3. TESTS AND RESULTS

3.1. *Solid half-cylinder in water*

The results of two boiling runs using the solid half-cylinder and a single run using air bubbles are shown in Fig. 4. The air flow rate of 1–3 l min^{-1} provided approximately the same total gas bubble volume around the tube to that which occurred in boiling alone at 100 kW m^{-2}. Thus, it would appear that at this heat flux about half of the heat transfer was due to the bubble turbulence. Two zones can be defined: one where the heat transfer due to the bubbling gas is a strong function of the gas flow rate, and two where a maximum is reached and further increase only

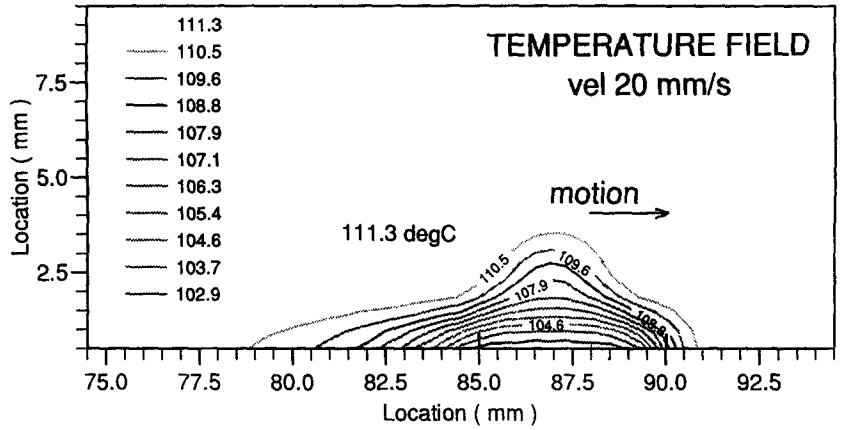

Fig. 2. Metal shim temperature contours for a 5 mm diameter bubble in steady flow at 20 mm s^{-1}.

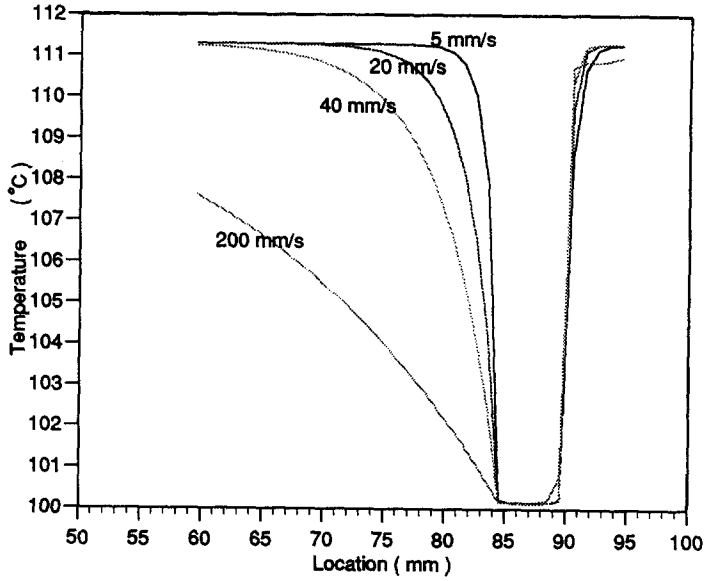

Fig. 3. Influence of velocity on the metal shim temperature profile.

occurs in the evaporative part. Most industrial systems operate at heat flux well into the second zone.

3.2. *Local mechanism under shim using water*

Two sequences of bubble growth and sliding departure are studied in this subsection. They are selected from several hours of HSVC tape recording and characterize the mechanisms observed under our conditions in water. These conditions are essentially boiling in tap water at 100°C at a heat flux of 7.0 kW m^{-2} after taking account of losses from the electrically heated shim.

Differential error analysis indicates probable errors in absolute values of temperature difference up to 30% owing to the translation from video recording to hue estimation and then to isotherms. However, we are primarily concerned with relative effects where the errors will be around 10%. It is recognized that determination of heat transfer and simultaneous visualization in this difficult geometry can only lead to approximate data and they should be treated as such.

Sequence I results are summarized in Figs. 5–7 and show a sketch of the processes involved, the thermal contours from the hue analysis and the temperature–time history at three selected positions identified as points 3, 5 and 6. Comparative scrutiny of these figures allows a clear picture of the bubble movements and growth. Bubble C was the only one to clearly arrive from below rather than from nucleation on the surface and growth and movement from arrival at the

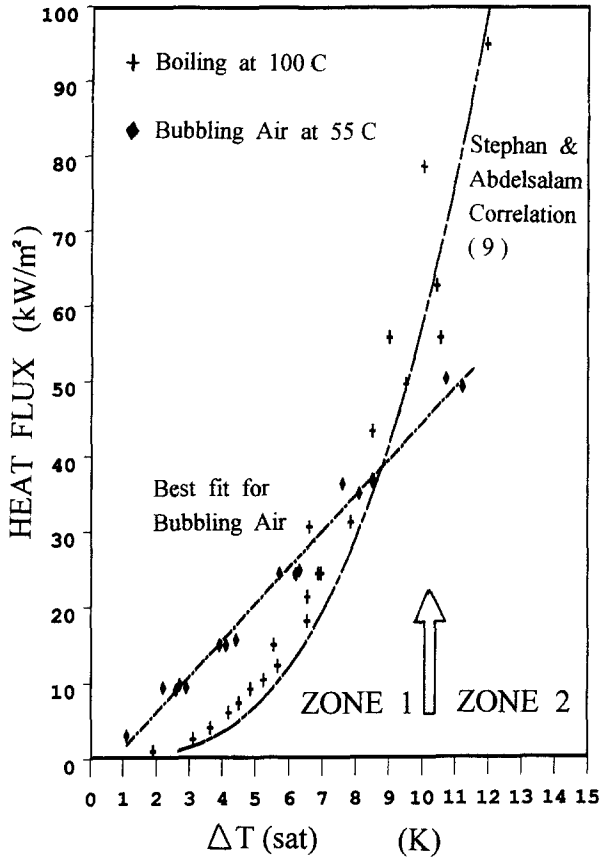

Fig. 4. Heat transfer due to bubbling air and boiling in water under the half cylinder.

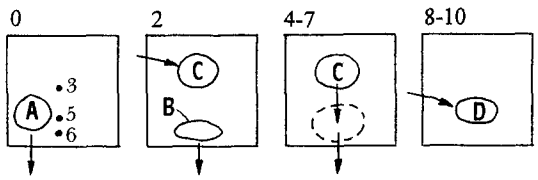

Fig. 5. Schematic of sequence I for a 14 mm² area at the base of the shim over a 10 s period.

tube to sliding and departure is well-defined. The clear temperature rise of the surface of up to 11°C above T(sat) under the bubble should be noted for our subsequent discussion.

Sequence II covered by Figs. 8–11 shows a similar set of results for a more complicated period involving about 10 bubbles. The points 1 and 3, for which time histories are plotted, cover bubbles M, P, R and T. It should be noted that bubble P influences point 3 although it departs from a position several millimetres away owing to the bubble sweeping over the position. The very high temperatures in the centres of bubbles P and T are really outside the range of the paint and are accordingly shaded in by hand in the hue plots of Fig. 9.

3.3. *Local mechanism under shim using Flutec PP1*

Some similar tests were conducted using Flutec PP1 ($C_{10}H_{12}$) rather than water as mentioned earlier. The boiling point of 57°C is suitably covered by one of the commercial thermochromic paints (Radio Spares, UK) which changes from red through to blue over the range of about 60–80°C. It was observed that the bubbles remained at the surface for a very short time (<0.5 s) during which they grew to a size of about 2 mm diameter. Clear identification of the bubbles using the surface colour change and the direct image was unreliable with the present HSVC and experimental apparatus.

Careful observation of the video tapes of this process does however show small red smears on the yellow/green background. These smears correspond to small bubbles sliding over the surface and since red indicates a temperature <61°C in a background of around 65°C, there is very definitely a drop in temperature owing to the passage of these bubbles. This is in marked contrast to the rise in temperature under

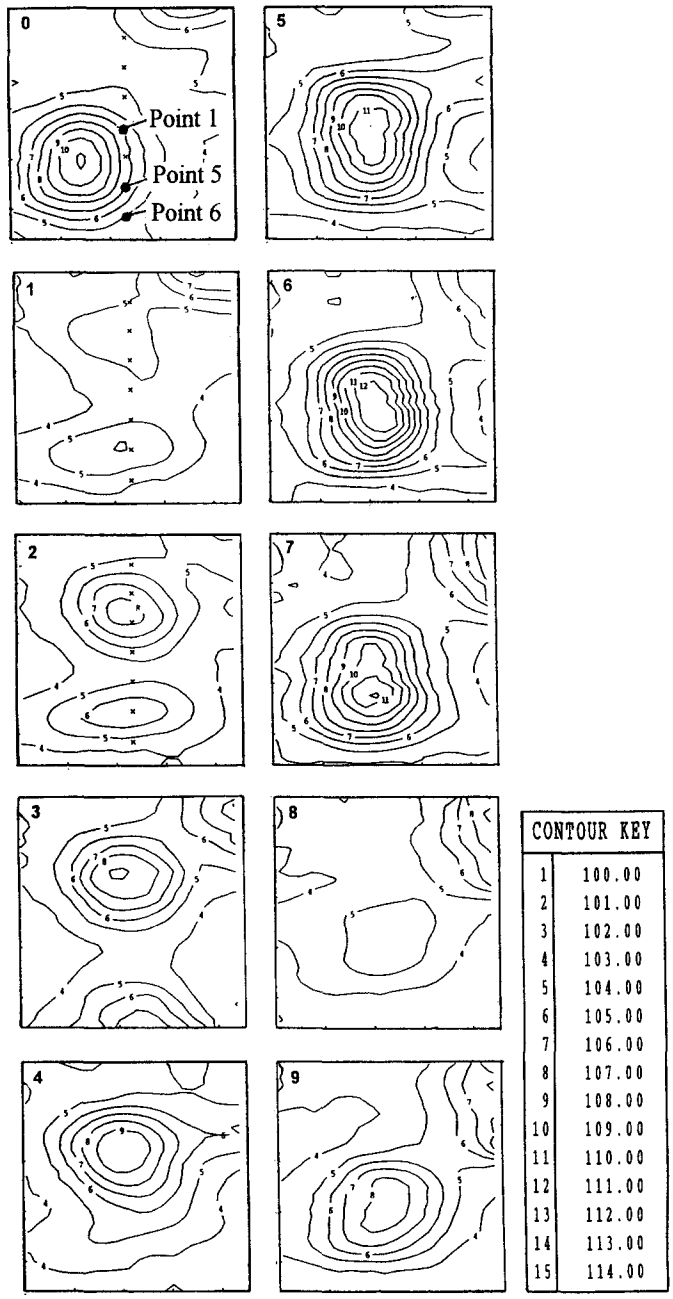

Fig. 6. Hue contours for sequence I over 10 s.

the large and slow-moving water bubbles. Proper evaluation of organic fluids needs a rig allowing pressurization and faster video equipment with close-up viewing facilities.

4. CONCEPTUAL CONSIDERATIONS AND DISCUSSION

4.1. *Mean heat transfer rates*

As mentioned earlier, our work on heat transfer under boiling, condensing and air bubbling conditions to a single tube in a bundle of tubes has established the importance of both the turbulent and evaporation mechanisms. However this work used R113 and the influence of other working fluids was unclear.

The results shown in Fig. 4 clearly indicate a similar pattern for water under conditions of boiling under a tube. The boiling heat fluxes in water are of course higher than those of common refrigerants and organics. If account is taken of the six times difference in critical heat flux between water and R113 (at 1 atm), the close comparison of these results at 100 kW m^{-2} and those for boiling R113 at 15 kW m^{-2} in ref. [3] is to be expected. In both cases, a substantial proportion

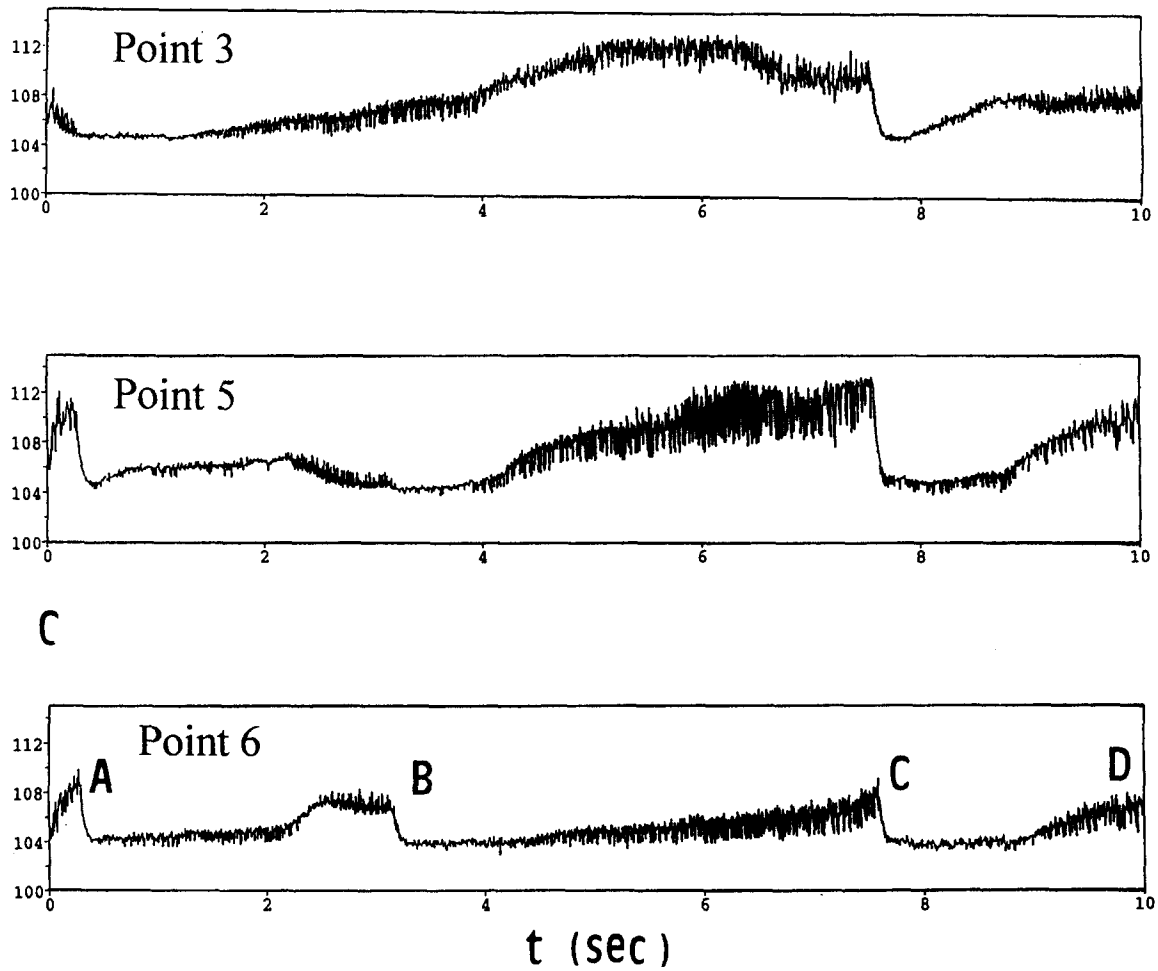

Fig. 7. Temperature profiles for points in sequence I.

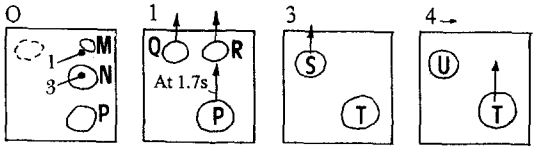

Fig. 8. Schematic of sequence II for a 14 mm^2 area at the base of the shim over a 5 s period.

of the heat transfer was due to turbulence caused by the bubbles rather than evaporation at the surface.

4.2. *Heat transfer under the large bubbles in water*

It is difficult to explain the large surface temperature rises found in the growing bubbles under the shim unless it is assumed that a dry patch develops. The following simple analysis adds corroborative evidence to this assumption. The radial temperature distribution in the thin stainless-steel surface under the bubble may be treated as pseudo-steady state as, for the experimental conditions, the bubble is present for a few seconds and temperature equilibrium in the metal layer occurs in less than a millisecond. Heat flow in the layer can therefore be approximated to radial heat generation with the contact radius r_c increasing with time as shown in Fig. 11. If heat flow at the surface of the layer is taken as zero except where in contact with the liquid and the temperature at r_c and beyond is taken as T_c, then the radial conduction equation:

$$r\frac{\partial^2 T}{\partial r^2}+\frac{\partial T}{\partial r}=-\frac{q_g r}{k} \tag{1}$$

becomes

$$T=\frac{q_g}{4k}(r_c^2-r^2)+T_c. \tag{2}$$

Under the test conditions during which sequence I and II were conducted at 14.3 A:

$$q_g=\left(\frac{I}{A}\right)^2\rho=344\times10^3\ \text{kW m}^{-3}. \tag{3}$$

The temperature difference ΔT_c of the centre of the

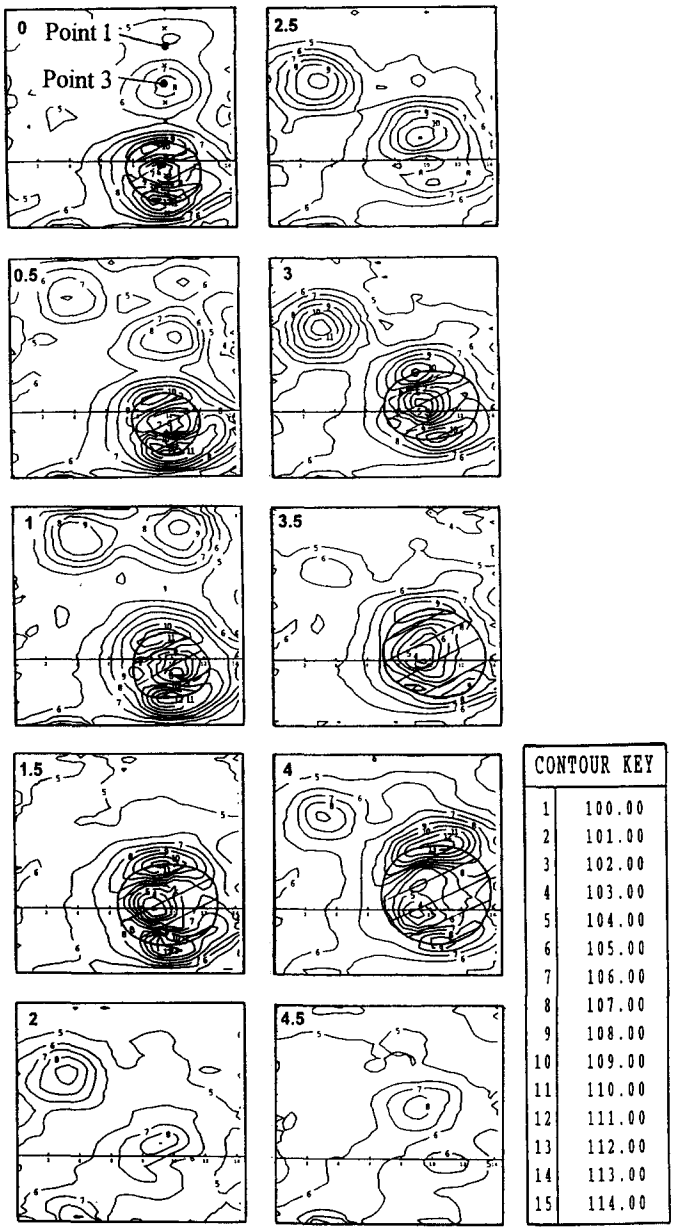

Fig. 9. Hue colours for sequence II over 5 s.

layer under the bubble ($r = 0$) above T_c is given (with $k = 16 \times 10^{-3}$ kW mK^{-1}):

$$\Delta T_c = 5.38 \times 10^6 r_c^2 \quad (4)$$

With r_c in the sequences typically around 1–2 mm, this yields ΔT_c in the range 5–20°C.

This correlates well with the experimentally determined differences between the centres and the edges of the dry spots of up to 8°C. The experimental sensitivities and unknown temperatures at r_c render more sophisticated analysis untenable. However, this analysis does provide strong evidence that the centre of the bubble has dried out and consequently that high heat transfer occurs beyond the liquid–contact radius.

Furthermore, study of the sequences shows that this dry spot can move (bubble C) and can seed a further bubble after departure (bubble D) although on other occasions a bubble may arise nearby when one would expect some seeding (say S from Q). Even as the bubble slides along after departure there can be a rise of temperature (P at point 3) when one may expect a layer of liquid and a lower temperature. It does appear that the mechanisms are multifarious and do not lend themselves to easy analysis.

4.3. *Heat transfer under the small bubbles in Flutec*

The complex flow and heat transfer mechanisms are apparently strongly influenced by the working fluid.

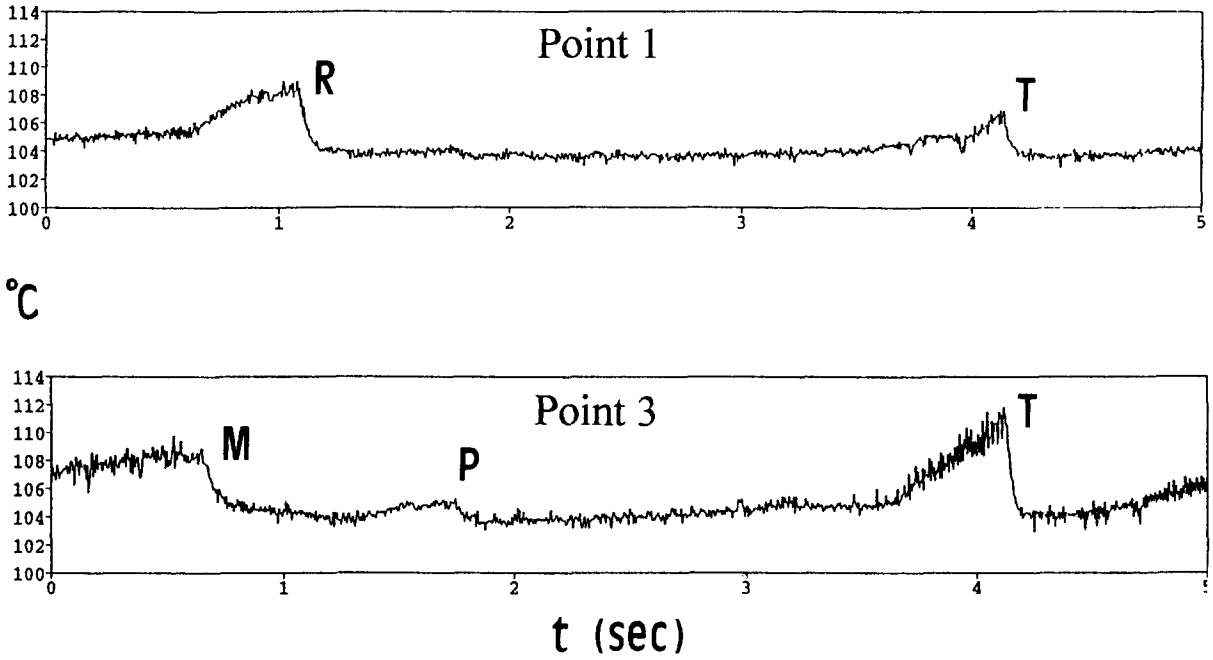

Fig. 10. Temperature profiles for points in sequence II.

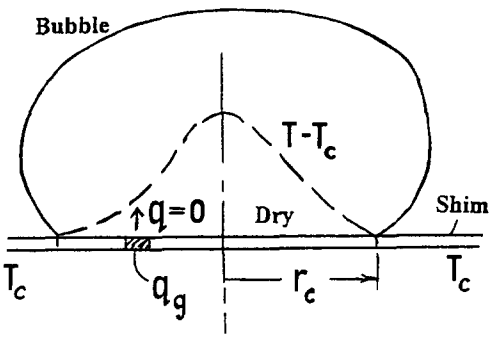

Fig. 11. Model of shim and bubble with dry patch.

As already seen from attempts to run the tests with Flutex PP1, the bubbles slide past the surface leading to a decrease in the surface temperature. Whether this is due to brushing away the boundary layer or the presence of a thin evaporating layer under the bubble, or both, is difficult to ascertain.

Current work (Addlesee and Cornwell [7]) on the hydrodynamic layer thickness under a sliding bubble shows that the thickness is primarily a function of fluid viscosity, bubble geometry and velocity. The layer thicknesses for bubbles under the shim for the water and Flutec under the conditions of our experiments are around 150–200 μm, respectively. This would lead to very little evaporation of the layer as evaporation requires thicknesses a factor of ten times lower [8]. This implies that the low-temperature streaks seen in the Flutec boiling tests are caused by disturbance of the liquid boundary layer alone.

5. CONCLUSIONS

This study has demonstrated that there are no unique answers to questions regarding the existence or otherwise of a thin layer under a sliding bubble. In the case of water, bubbles may pass close to the surface and receive heat from the outer reaches of the boundary layer or may penetrate the layer and lead to a dry spot so that the bubbles are captured until growth and buoyancy eventually act to draw them away. In the case of Flutec, the bubbles were much smaller and no dry spots were detected.

It is concluded that neither the bubble-sweeping mechanism nor the layer-evaporation mechanism is dominant under all conditions and that both must be included in any analysis of the local heat transfer. Where the mean heat transfer from a tube in a bundle is concerned it well explains why the bubbly-flow in the upper part of bundle leads to higher heat transfer coefficients.

Acknowledgements—The authors are indebted to Dr Y. Yan of the Department of Engineering Sciences, Oxford University for the hue analysis of the high-speed video recording. The work was supported by the Engineering Physical Sciences Research Council on Grant GR/H45377.

REFERENCES

1. Cornwell, K., The role of sliding bubbles in boiling on tube bundles. In *Heat Transfer* 1990 (9th International Heat Transfer Conference, Jerusalem). Hemisphere, New York, 1990, pp. 455–460.
2. Cornwell, K., Houston, S. D. and Addlesee, A. J., Sliding bubble heat transfer on a tube under heating and cooling

conditions. In *Pool and External Flow Boiling*, Engineering Foundation Conference, Santa Barbara, ASME, NY, 1992, pp. 49–53.
3. Houston, S. D. and Cornwell, K., Heat transfer to sliding bubbles on a tube under evaporating and non-evaporating conditions. *International Journal of Heat and Mass Transfer*, 1996, **39,** 211–214.
4. Nashikawa, K., Fujita, Y., Uchida, S. and Ohta, H., Effect of surface configuration on nucleate boiling heat transfer. *International Journal of Heat and Mass Transfer*, 1984, **27,** 1559–1571.
5. Tong, W., Simon, T. W. and Bar-Cohen, A., A bubble sweeping heat transfer mechanism for low flux boiling on downward facing inclined surfaces. *ASM Heat Transfer Digest*, 1988, **104,** 173–178.
6. Yan, Y. and Kenning, D. B. R., Heat transfer near sliding bubbles in boiling. In *Heat Transfer* 1994, 10th International Heat Transfer Conference, Brighton, U.K. Hemisphere, New York, 1994, pp. 195–200.
7. Addlesee, A. J. and Cornwell, K., Liquid film thickness above a bubble rising under an inclined plate. *Trans IChemE*, 1997, **75A,** 663–667.
8. Cornwell, K. and Schuller, R. B., A study of boiling outside a tube bundle using high speed photography. *International Journal of Heat and Mass Transfer*, 1981, **25,** 683–690.
9. Stephan, K. and Abdelsalam, M., Heat transfer correlations for natural convection boiling. *International Journal of Heat and Mass Transfer*, 1980, **23,** 73–97.